A Coaxial, Three-Coil Probe for Measuring Local Values of Electrical Conductivity and Velocity in Plasma Streams

EDWARD W. VENDELL*
Utah State University, Logan, Utah
AND
RUDOLPH E. POSCH† AND GEORGE R. COOK†
NASA Ames Research Center, Moffett Field, Calif.

A primary coil excited by 100 kHz current is located between two secondary sensing coils. In an axisymmetric plasma stream with magnetic Reynolds numbers less than unity, changes in the induced sum and difference voltages are simultaneously detected and linearly related to local values of conductivity σ and velocity U by means of an analysis based on Ohm's law and Maxwell's equations. In electrolytes σ was within 5% of standard conductivity cell readings for four probe models having different outside diameters (4 mm minimum) and coil spacings (1.14 cm minimum). Each probe was tested in a free, 16.5-cm-o.d., argon plasma jet that was created as the gas expanded from 1.0 to 5 $\times$ 10^{-4} atm through a 1.27-cm-diam constricted arc. The resulting measured centerline values of σ ranged from 300 to 900 mho/m whereas the corresponding values of U varied from 3.5 to 8 km/sec and agreed within 8% of independent values computed from flow-swallowing mass and enthalpy probes. Although test Mach numbers ranged from 3 to 6, the effect of possible oblique shocks was negligible since the probe Knudsen numbers were near unity. Corrections calculated from theory for stream diameter and finite probe size were small and brought the results from the various probe sizes into closer agreement.

Nomenclature

$\mathbf{b}_t, \mathbf{b}_U$ = perturbation magnetic field due to conductivity and velocity, w/m
$\mathbf{B}$ = magnetic field, w/m
d = spacing between coils, m
G = amplifier-filter gain
I_p = current through primary, A
K = correction factor for finite probe size
m = dipole moment of primary coil
n = number of turns on a coil
r = distance from primary to field point; with subscript, radius of coil
$R; R_m$ = radius of stream; magnetic Reynolds number
U = velocity of stream
θ = correction factor for position in finite stream
μ = magnetic permeability; 1.26×10^{-6} H/m
ρ = radial distance from axis of cylindrical stream to probe
$2\rho_0$ = diameter of probe
σ = electrical conductivity
Φ = output voltage
$\omega/2\pi$ = frequency of primary current

Subscripts

p = primary
s = secondary
Σ = conductivity
Υ = velocity
∞ = unbounded media
1 = coil 1
2 = coil 2

Presented as Paper 69-327 at the AIAA 4th Aerodynamic Testing Conference, Cincinnati, Ohio, April 28–30, 1969; submitted September 17, 1969; revision received January 22, 1970. The major portion of this investigation was completed at the NASA Ames Research Center, Moffet Field, Calif. and was supported at the Utah State University under NASA Grant NGR-45-002-011. The authors gratefully acknowledge the aid of J. R. Jedlicka, V. Kirna, V. J. Rossow, and the personnel of the Magnetoplasmadynamics Branch of the Ames Research Center.

* Associate Professor, Mechanical Engineering. Member AIAA.
† Research Scientist.

Introduction

IN the design and testing of arcjet facilities, hypervelocity wind tunnels, and magnetohydrodynamic (MHD) generators and accelerators, two plasma properties are of considerable importance in the evaluation of the efficiency of such a device: electrical conductivity and mass-average stream velocity. For example, conductivity and velocity profiles taken at the exit of an MHD accelerator could be used to determine the effectiveness of seeding gases and to optimize the spacing and location of electrodes. Furthermore, since the values of two independent intensive properties are sufficient to determine the thermodynamic state of an equilibrium plasma, a conductivity profile and, say, a temperature profile could be used with appropriate formulae to obtained local values of other properties such as electron density or average electron collision frequency.

Although many methods of conductivity and velocity measurement have been proposed, the immersible three coil instrument designed by Rossow and Posch[1] is the only one known to the authors that simultaneously records local values of conductivity and velocity which are based on calibration in room air and simple linear equations derived from the fundamental equations of physics. Reference 2 contains a comprehensive review of other methods.

The theoretical and experimental work presented in Ref. 1 contains equations in closed form for an oscillating dipole magnetic field in an unbounded medium and for eddy current perturbations due to the conductivity and velocity of the medium. Also given are experimental results for a threesting three-coil probe that are in good agreement with theory. The work was extended by Vendell,[3] who developed theoreti-

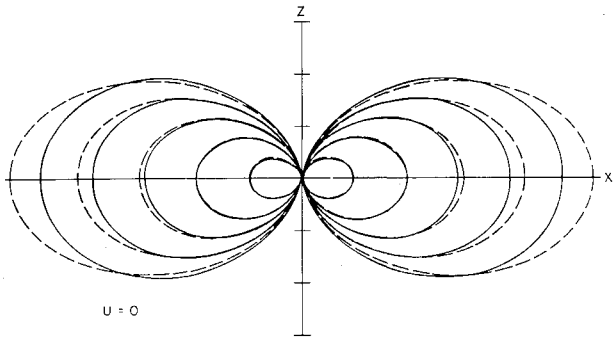

Fig. 1a Primary dipole field, $\mathbf{B}_p$, in room air (——) and perturbed field (- - -), $\mathbf{B}_p + \mathbf{b}_t$, in a quiescent conducting fluid having a magnetic Reynolds number $R_{mt} = 0.4$.

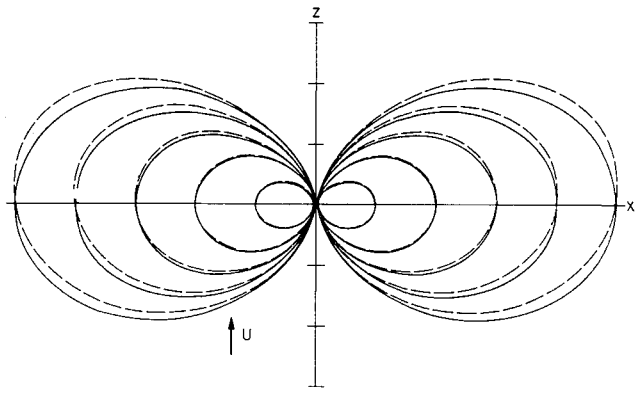

Fig. 1b Primary dipole field, $\mathbf{B}_p$, in room air (——) and perturbed field (- - -), $\mathbf{B}_p + \mathbf{b}_U$, in a moving conducting fluid having a magnetic Reynolds number $R_{mU} = 0.4$.

cal corrections for the case where the probe is axially located at any radial position in a cylindrically bounded stream.

In the present work, a new instrument is described in which the three coils are coaxially positioned inside a single sting so that stream disturbance is significantly reduced. The new probe is easier to assemble, is more rugged, and the cylindrical boundary corrections presented below are smaller than for the previous design.

Theory

The theory developed in Ref. 1 is based on the application of Maxwell's equations and the simplified Ohm's law for moving conductive fluids. Sinusoidal current at 100 kHz flows in a primary coil creating a dipole magnetic field, $\mathbf{B}_p$. In an electrically conducting quiescent fluid, this field induces eddy currents having an associated perturbation magnetic field $\mathbf{b}_t$. Similarly, when a conducting fluid moves past the primary magnetic field parallel to the dipole axis (z axis), currents are induced having an associated perturbation magnetic field $\mathbf{b}_U$. For this problem two magnetic Reynolds numbers have been defined: $R_{mt} = \sigma\mu\omega r_p^2$ and $R_{mU} = \sigma\mu U r_p$, where $\mu = 1.26 \times 10^{-6}$ H/m, ω is the sinusoidal angular frequency of field variation, and r_p is the characteristic radius of the primary coil. If each of these Reynolds numbers is less than one, then the uncoupled perturbations $\mathbf{b}_t$ and $\mathbf{b}_U$ can be represented in closed form and the total field can be represented by a series expansion in the magnetic Reynolds numbers of the form $\mathbf{B} = \mathbf{B}_p + \mathbf{b}_t + \mathbf{b}_U + \mathbf{O}(R_{mt}^2, R_{mU}^2) + \ldots$ where the primary field $\mathbf{B}_p$ is a zeroth order term, $\mathbf{b}_t$ and $\mathbf{b}_U$ are first-order terms in R_{mt} and R_{mU}, respectively, and terms of second order and higher are small enough to be neglected

Examples of the typical orientation of magnetic field line of an oscillating dipole in room air and for the total field including perturbations in the presence of a conducting stationary and conducting moving fluids are shown in Figs. 1a and 1b, respectively. In these cases the magnetic Reynolds numbers are $R_{mt} = 0.4$ and $R_{mU} = 0.4$.

The magnetic field perturbations can be detected by measuring changes in the induced voltages of suitably placed sensing coils. In Ref. 1 the induced voltages due to the impressed primary field were eliminated by a suitable choice of the orientation and position of the sensing coils so that the perturbation fields created coil voltages that were linearly and independently related to σ and σU.

The analysis of Rossow and Posch is based on the following restrictive assumptions. 1) The conductive fluid has associated magnetic Reynolds numbers each less than unity. For the tests discussed here, neither of the two magnetic Reynolds numbers was ever greater than 0.05. 2) Flow disturbances of the plasma stream because of the presence of the probe are negligible. This assumption is reasonable in the present work because the minimum Knudsen number attained during testing was estimated to be 0.782. 3) Flow disturbances due to primary dipole magnetic pressures are much less than stream pressures. In the present tests, magnetic pressures were about 10^{-6} atm, while dynamic stream pressures were about 0.02 atm. 4) The primary coil dimensions and the spacing of sensing coils are such that the primary can be considered to be a dipole. 5) Displacement and Hall currents are negligible. 5) The plasma is neutral everywhere. For the results reported herein the debye length was estimated to be $< 6 \times 10^{-6}$ m, a value that is considerably smaller than any probe dimension. 7) The frequency of the applied magnetic field is well below the plasma frequencies of either the plasma or the electrolytes, both of which were greater than 10^{10} Hz. 8) Conductivity can be represented as a scalar. This assumption is reasonable because the primary magnetic field in the present tests was $< 10^{-6}$ w/m. 9) The conductivity and velocity are uniform. 10) The flowfield is unbounded. Restrictions 9 and 10 can be removed by corrections calculated by Vendell[3] based on a numerical analysis of magnetic images.

One of the various means suggested in Ref. 1 for measuring σU was a coaxial arrangement of a primary dipole and two flanking sensing coils. The voltage output difference of the secondary coils was linearly related to σU whereas the sum of the output voltages was linearly and independently related to σ. The advantages of such a single sting device led the authors to develop a circuit that would simultaneously and independently record these sum and difference voltages.

According to Ref. 1, the z components of the magnetic fields at any field point (x,y,z) created by an n_p-turn dipole whose axis is in the z direction, and whose center is located at $(x,y,z) = (0,0,0)$ are as follows:

$$B_p = -m\cos\omega t[(3z^2/r^2 - 1)1/r^3] \quad (1)$$

$$b_t = -(\sigma\mu\omega m \sin\omega t/2)[(r^2 + z^2)/r^3] \quad (2)$$

$$b_U = (\mu\sigma U m \cos\omega t/2)(1 - 3z^2/r^2)(z/r^3) \quad (3)$$

where

$$r = (x^2 + y^2 + z^2)^{1/2},\ m = n_p r_p^2 \mu I_p/4 \quad (4)$$

and r_p is the characteristic coil radius. The voltage Φ_s induced in each sensing coil is

$$\Phi_s = -\pi n_s r_s^2(\partial/\partial t)(B_p + b_t + b_U) \quad (5)$$

where n_s represents the number of coil turns.

If sensing coil no. 1 is located at $(x,y,z) = (0,0,d)$ and no. 2 at $(x,y,z) = (0,0,-d)$, and if $n_1 = n_2 = n_s$, $r_1 = r_2 = r_s$, then Eqs. (1–5) imply that

$$\Phi_1 = -\pi n_s r_s^2 m\omega\left(\frac{2\sin\omega t}{d^3} - \frac{\sigma\omega\mu\cos\omega t}{d} + \frac{\sigma U\mu\sin\omega t}{d^2}\right) \quad (6)$$

$$\Phi_2 = -\pi n_s r_s^2 m\omega\left(\frac{2\sin\omega t}{d^3} - \frac{\sigma\omega\mu\cos\omega t}{d} - \frac{\sigma U\mu\sin\omega t}{d^2}\right) \quad (7)$$

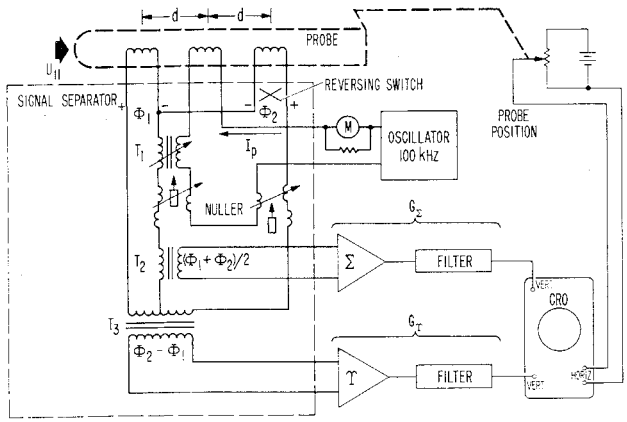

Fig. 2 Schematic of probe, signal separator, and associated equipment.

The circuit shown in Fig. 2 is capable of displaying the difference and the average of Φ_1 and Φ_2 independently and simultaneously on the screen of a dual-beam cathode ray oscilloscope. Equations (6) and (7) may be used to obtain these values with the result that

$$\Phi_2 - \Phi_1 = M\sigma U\mu \sin\omega t/d^2 \tag{8}$$

$$(\Phi_1 + \Phi_2)/2 = M(-\sin\omega t/d^3 + \sigma\mu\omega \cos\omega t/2d) \tag{9}$$

where

$$M \equiv 2\pi n_s r_s^2 m\omega \tag{10}$$

Equation (9) suggests that if a voltage of magnitude

$$+\frac{M \sin\omega t}{d^3} \tag{11}$$

is applied to transformer T_1, then the output of T_2 will be zero in room air ($\sigma = 0$) and the signal entering the Σ-amplifier will be a function of σ only. The voltage defined by expression (11) can be measured by temporarily reversing the leads of coil no. 2 so that the voltage appears at T_2. If G_Σ is the combined gain of the summing (Σ) amplifier and filter, then the peak voltage at the readout is

$$\Phi_{cal} = G_\Sigma(M/d^3) \tag{12}$$

This relationship will be used below to eliminate the parameter M.

With the probe leads in normal position so that when U is zero, the output of T_3 is zero, the peak value of $\Phi_2 - \Phi_1$ at the readout after filtering and amplification by the differencing-amplifier (Υ) is

$$\Phi_{\gamma\infty} = G_\gamma M\mu\sigma U/d^2 \tag{13}$$

where subscript ∞ refers to unbounded media and G_Υ is the combined gain of the amplifier and filter. After the signal contribution due to B_p has been eliminated, the peak value of $\Phi_1 + \Phi_2$ at the output of the other amplifier-filter is

$$\Phi_{\Sigma\infty} = G_\Sigma M\mu\omega\sigma/2d \tag{14}$$

Eqs. (13) and (14) are the expressions for the voltages that would be produced by an infinitesimal probe immersed in a uniform unbounded fluid.

Vendell[3] has used the method of magnetic images to calculate corrections for finite stream size and off-axis probe location for uniform streams. When his method is applied to the coaxial probe, graphs of the correction factors $\theta_\Sigma = \Phi_\Sigma/\Phi_{\Sigma\infty}$ and $\theta_\Upsilon = \Phi_\Upsilon/\Phi_{\Upsilon\infty}$ are obtained as functions of d/R and ρ/R, where d = coil spacing, R = radius of stream, ρ = radial position of probe, and Φ_Σ and Φ_Υ refer to signals recorded in uniform cylindrically bounded streams. Figures 3 and 4 give

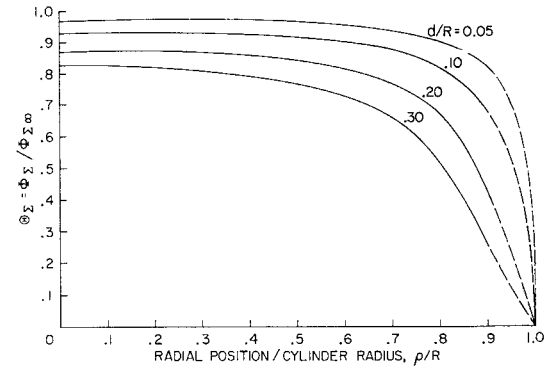

Fig. 3 Theoretical conductivity boundary correction factors for cylindrical streams. Dashed lines represent extrapolations.

graphical values of the boundary correction factors for conductivity θ_Σ and for conductivity-velocity θ_Υ, respectively. If these factors are applied to Eqs. (13) and (14), then the signals that would be expected in a bounded uniform fluid are

$$\Phi_\Upsilon = \theta_\Upsilon G_\Upsilon M\sigma U/d^2 \tag{15}$$

$$\Phi_\Sigma = \theta_\Sigma G_\Sigma M\mu\omega\sigma/2d \tag{16}$$

Equations (15) and (16) may be combined to yield

$$U = \theta_\Sigma G_\Sigma \Phi_\Upsilon \omega d/2\theta_\Upsilon G_\Upsilon \Phi_\Sigma \tag{17}$$

and the combination of Eqs. (12) and (16) gives

$$\sigma = 2\Phi_\Sigma/\theta_\Sigma\mu\omega d^2\Phi_{cal} \tag{18}$$

In order to correct for the absence of perturbation currents in the volume occupied by the probe itself, an integral discussed in Ref. 1 has been applied to the coaxial probe geometry to give the ratio of actual U and σ to apparent U and σ as a function of the ratio of probe diameter, $2\rho_0$, to coil spacing d. These ratios K_Υ and K_Σ are presented in graphical form in Fig. 5. Thus Eqs. (17) and (18) become

$$U = K_\Upsilon\theta_\Sigma G_\Sigma \omega d\Phi_\Upsilon/2\theta_\Upsilon G_\Upsilon \Phi_\Sigma \tag{19}$$

and

$$\sigma = 2K_\Sigma\Phi_\Sigma/\theta_\Sigma\mu\omega d^2\Phi_{cal} \tag{20}$$

Equations (19) and (20) give conductivity and velocity values that are fully corrected for finite probe and stream size and these expressions were used to reduce the data presented below.

Figures 3 and 4 indicate that θ_Σ and θ_Υ are nearly equal to unity for small values of d/R except near the edge of the cylindrical boundary. Since the value of d/R was less than

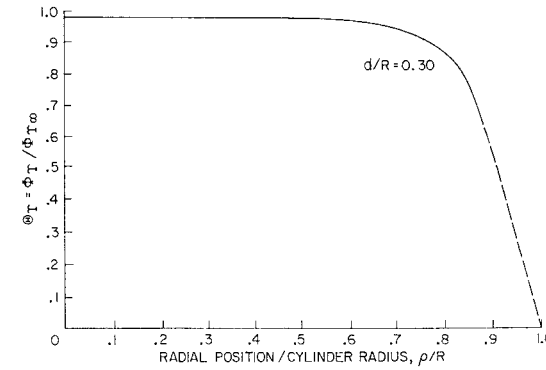

Fig. 4 Theoretical conductivity-velocity boundary correction factors for cylindrical streams. Dashed line represents an extrapolation.

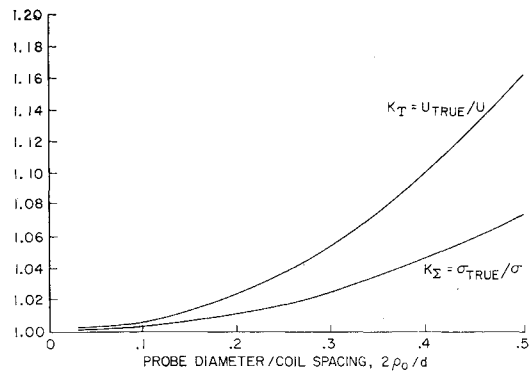

Fig. 5 Correction factors for finite probe size.

0.3 for all plasma data presented herein, θ_T was taken to be unity in Eq. (19).

Apparatus

Figure 6 is a cross section of a typical probe used in this series of tests. Coils were wound on polycarbonate forms positioned on a quartz center rod and then inserted in a quartz tube that acted as a heat shield. Each coil was wound to give a desired Φ_{cal}. In the smallest probe, for example, there were 200 turns of no. 40 AWG Formvar wire wound on each form. It was necessary to shield the probe against capacitive coupling, especially in the tests in electrolytes. This was accomplished with another layer of enameled wire, which, having no large closed loops, did not form field-disturbing eddy currents. The probes varied in length from 4 to 8 in. and it was found that about five coil widths from sensing coil no. 1 to the tip of the heat shield was sufficient to insure fore-and-aft symmetry with respect to the center of the primary coil so that the σ and σU signals were independent of each other. The probe was mounted on an 11-in. pivoted arm which swept the probe through the stream by means of a hydraulically driven rack and pinion. Attached to the pivot was a single-turn potentiometer, the output of which controlled the horizontal sweep of the oscilloscope as shown in Fig. 2.

The signal separator shown in Fig. 2 was designed to accommodate probes having a given Φ_{cal} range. Capacitively and inductively balanced, shielded, twisted pairs were used throughout the circuit and the probe primary coil was wound bifilarly with a grounded center. Coarse and fine nulling devices were included in both the center leg and one of the side legs. Fiberboard tubing provided the forms on which a single turn primary lay between two oppositely wound coils (three turns each) on slightly larger tubing so that the sensitivity of the nulling device could be varied by changing the spacing between the primary and the two secondaries. Two pairs of differential nulling coils connected in series in each leg are represented by the single pair in each leg in Figs. 2. Voltages in one pair in each leg were changed with a ferrite slug and in the other pair in each leg with a steel slug. The ferrite slug changed signal amplitude at 0° or 180° phase and the steel slug changed amplitude at about 70° or 250° phase. Hence, an almost complete amplitude and phase adjustment was possible. For finer in-phase adjustments, a brass slug

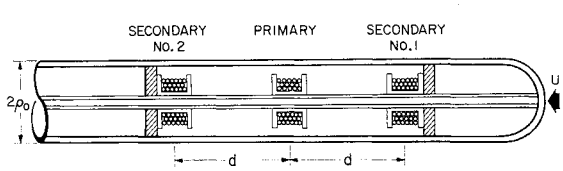

Fig. 6 Three-coil coaxial probe.

Table 1 Probe characteristics and dimensions

Parameter	Probe designation A	B	C	D
Probe diameter, $2\rho_0$, cm	1.03	1.03	1.03	0.42
Coil spacing, d, cm	1.91	2.54	3.18	1.14
Calibration signal, ϕ_{cal}, mv[a]	192.0	108.0	18.0	22.5

[a]This value appears at the filter output when the probe is in room air.

was used in another nulling device in series with the first. Transformer T_3 was wound bifilarly and differentially so that the impedance from each leg to the center was very low for σ signals. The impedance of transformer T_2 was high compared to all other impedances. Although for our purposes it was not necessary, we could have made the separation unit even more independent of impedance changes in the probe by proper choice of capacitance across inputs of transformers T_2 and T_3, thereby increasing the input impedance of the separation unit by resonating the circuits.

As indicated in Fig. 2, a crystal controlled oscillator supplied $\frac{1}{8}$ w at a frequency of 100 kHz to the primary coil of the probe. Voltages from the signal separation transformers were fed through amplifier-filter units each having a gain of 10 and read out by a dual trace cathode ray oscilloscope having a maximum sensitivity of 10 μv per division. The magnetostrictive filters had a bandpass of 100 Hz. Current to the probe was monitored to insure that the probe was operating with the same current that was used for calibration. The linearity of the amplifiers and the constancy of the readout system were checked periodically by means of a standard attenuator.

Experimental Results in Electrolytes

Table 1 is a summary of some parameters for the probes used in this experiment. The accuracy of each probe was checked by comparing the probe-determined conductivity [Eq. (20)] of various standard solutions of salt water or sulfuric acid using experimentally determined boundary corrections with the actual conductivity as determined by a standard conductivity cell. The latter consisted of a resistance measurement of electrolyte between two platinum electrodes powered by 1000 Hz current and gave values of σ which agreed well with the values given in the literature. The boundary corrections for the probe data were experimentally determined by recording centerline probe signals for several container sizes and extrapolating to infinite container size using the reciprocal of the container radius, as described in Refs. 1 and 3. For probes A, B, C, and D, standard cell values differed from extrapolated experimental values by −4.4, −8.5, −0.44, and +0.42%, respectively.

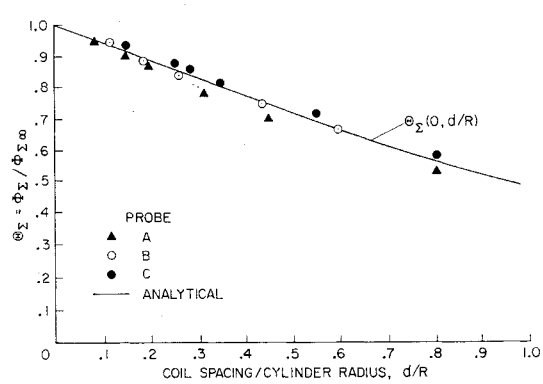

Fig. 7 Comparison of analytical and experimental centerline values of θ_Σ in electrolytes.

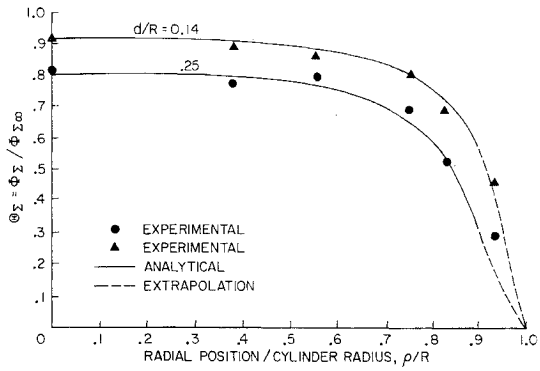

Fig. 8 Comparison of analytical to experimental values of θ_Σ at various radial positions in electrolytes.

The experimental verification of the theoretical centerline boundary correction factor θ_Σ is presented in Fig. 7 for several different container sizes and coil spacings. The experimental points were computed by forming the ratio of actual voltage to extrapolated voltage for infinite container size for different ratios of d/R.

Figure 8 is a similar comparison of θ_Σ with experimental values as a function of radial probe position for two different values of d/R.

Figures 7 and 8 indicate that the theoretical basis for the determination $\theta_\Sigma[(d/R), (\rho/R)]$ is valid in practice. No practical means for an experimental check of θ_T values has been devised.

Experimental Results in a Free Argon Plasma Jet

Each of the four coaxial probes was tested at various arc power settings in a low-density ($\sim 3.5 \times 10^{-5}$ kg/m^3) supersonic argon plasma jet created by the constricted arc facility described in Ref. 4. Each probe was swept through the 16.5-cm-diam stream in approximately 0.12 sec. Data records in the form of polaroid photographs were taken for each arc power setting and Fig. 9 is a typical photograph. The ordinates of the upper and lower traces are linearly related to σ and σU, respectively. The abscissa represents the radial position of the probe with respect to the center of the stream. The response of the instrument, evaluated by recording a sweep in both directions, on the same photo, as in Fig. 10, was found to be about 8 msec. This value was primarily a function of the bandwidth of the filters.

Examination of all the data records showed that there were no significant differences in the data with respect to sweep directions. Noise in the stream was found to be negligible when a powerless probe was swept through the stream. Nulls did not change because of heat flux (~ 2 kw/cm^2) in the larger

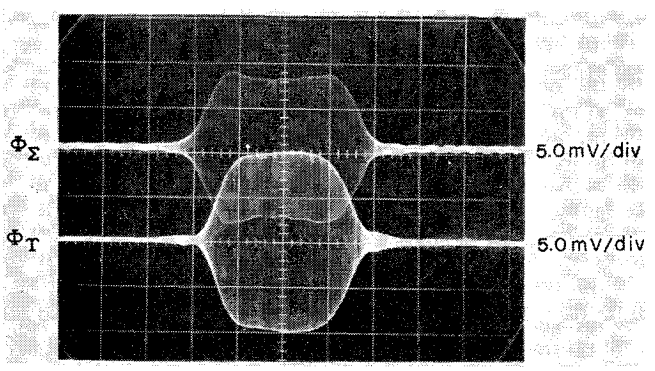

Fig. 9 A typical data record for Φ_Σ and Φ_T as recorded by probe A at an arc current of 500 A. In this case, σ_ℓ = 710 mho/m and U_ℓ = 5.35 km/sec.

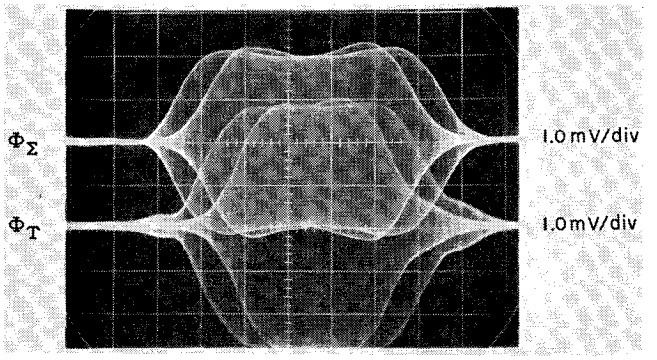

Fig. 10 A two-way sweep data record obtained by probe C at an arc current setting of 700 amps.

probes, but because of a larger surface-to-volume ratio, there was some drift of null in probe D. This small zero drift did not significantly affect the data. Some of the scatter in the data could be accounted for by the difficulty of getting repeatable arc current settings on the different days that tests were made.

The σ profiles of Figs. 9 and 10 confirm the observation of Emmons and Land,[5] that in many laboratory plasmas σ increases abruptly at the edge to an almost constant value in the interior of the jet. This fact was used to justify the assumption of uniform conductivity in the reduction of the probe data to obtain centerline values of σ. Similarly, σU was also assumed to be uniform, a convenience that is reasonable because Eq. (3) infers that the σU signal strength varies inversely as the square of the distance from the primary coil. These two assumptions are further discussed in a later paragraph.

Figure 11 presents centerline values of conductivity measured by the four probes on different days at various arc currents. These centerline data are based on the assumption of uniform conductivity and have been corrected for finite probe and stream size. With the exception of Probe A data, the results differed from probe-to-probe by less than 7% while the corresponding uncorrected values differed by as much as 25%. It was also found that data obtained with any given probe was repeatable within 5%, the same as the reading error.

Two sets of results for Probe C are presented in Fig. 11, the only difference being the diameter of the quartz heat shield. The agreement of these data suggests that the effects of possible oblique shocks and boundary layers were negligible. High-speed color film studies of several probe sweeps failed to indicate the presence of strong shocks. In addition, the data were not significantly affected by changing the heat-shield tips from hemispherical to 10° cone half-angle. Using measured values of centerline conductivity and static stream pressure as independent intensive thermodynamic variables,

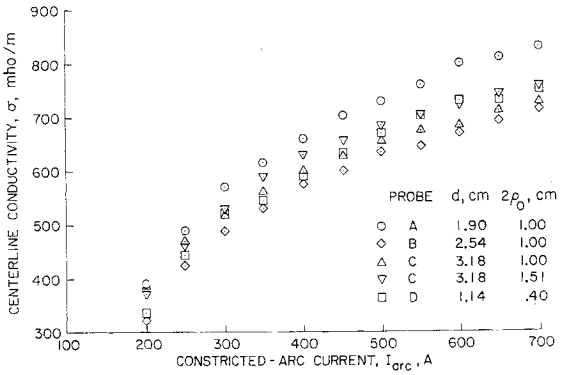

Fig. 11 Corrected centerline conductivity of a plasma stream for various arc currents, coil spacings d, and heat-shield diameters $2p_0$.

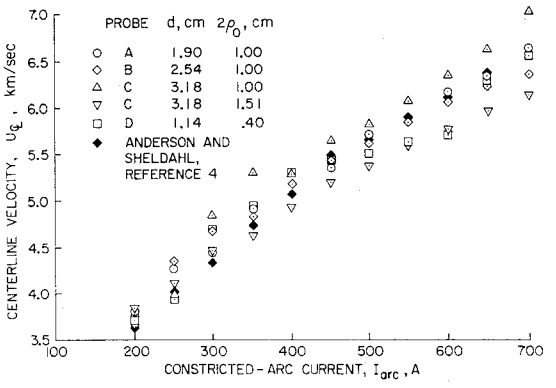

Fig. 12 Corrected centerline values of velocity of a plasma stream for various arc currents, coil spacings d, and heat-shield diameters $2p_0$.

values of the Knudsen number were computed from the theoretical equilibrium argon property values of Ahtye[6] resulting in a minimum value of 0.78. For all of these reasons it was concluded that all four probes were tested in the transition flow regime where shock and boundary-layer effects were negligible.

Unfortunately, no other independent measurements of plasma conductivity have been made in the same facility and electrolytes at normal temperatures and pressures do not have conductivity values high enough to bracket those of arc plasmajets. However, it should be emphasized that the calibration of the three-coil probe is independent of the properties of any conducting medium and it accurately predicts the conductivity of electrolytes in the 1.0 to 75 mho/m range with a maximum error of 8%.

In a given constricted-arc facility for a given gas (argon) and upstream reservoir pressure (1.0 atm), experimentally measured values of mass-average enthalpy, h_{AV}, at the exit plane may be plotted as a monotonic increasing function of constricted-arc current, I_{arc}.[7] Hence, if I_{arc} is known, one can determine h_{AV} which can be used with enlarged plots of Figs. 6 and 7 from Refs. 4 to obtain centerline velocity values that are plotted as a function of I_{arc} in Fig. 12 (see black diamonds). Also plotted on the same axes are corrected centerline velocity values measured by the four probes; these data are also based on the assumption of uniform σ and σU. As this comparison indicates, the largest disparity between the coaxial three-coil probe data and the independent measurements of Anderson and Sheldahl is about 8% at an arc current setting of 300 amps.

For several typical data profiles obtained with Probe D, σ and σU were assumed to be nonuniform and the corresponding centerline conductivity and velocity values were calculated according to a method described in detail by Vendell (Ref. 3, p. 19–26). This finite-increment technique yielded no important profile changes and produced centerline values of σ and U that differed from those computed on the basis of uniform σ and σU by less than 5%.

Because of the many possible uncertainty errors that enter into the various factors in the basic data reduction equations, Eqs. (19) and (20), a complete error analysis was not attempted. However, as noted previously, the largest conductivity error in electrolytes was 8.5% while the maximum centerline plasmajet velocity deviation from the independent measurements of Ref. 4 was about 8%. It should also be noted that Anderson and Sheldahl claim that the maximum error for their measurements of centerline velocity was 11%.

Conclusions

Probes for measuring conductivity and velocity of plasma streams were tested and showed good agreement with theory, each other, and independent means of conductivity and velocity measurement in electrolytes and an argon plasma, respectively. Numerical corrections calculated from theory were shown to be valid. Probes were immersible and were small enough to cause only a negligible disturbance in the low-density plasma streams. Data reduction was simple and could be automated for direct reading. For higher density streams, the authors plan to use probes with 10° conical tips to bring the shock wave closer to the probe body.

The probe can be used in streams having much higher conductivities and velocities by lowering the frequency of the primary coil power, at the same time maintaining the restrictions on the magnitude of the magnetic Reynolds numbers. Limitations on the application of the probe in other fluids is a function of the maximum feasible probe power, amplifier sensitivity, and filter bandpass. The minimum permissible stream radius is determined by the coil spacing and probe diameter, which, in turn, determine the heat sensitivity of the instrument.

As mentioned earlier, the probe system rise time varies inversely with the filter bandpass width. Since the magnitude of the random electromagnetic stream noise varies in different plasma facilities, the filter bandpass width should be varied until an acceptable rise time and filtering capability are achieved.

The use of the probe is now being extended to take measurements in a rocket exhaust plume as well as the exit stream of a MHD crossed-field accelerator.

References

[1] Rossow, V. J. and Posch, R. E., "Coil Systems for Measuring Conductivity and Velocity of Plasma Streams," *Review of Scientific Instruments*, Vol. 37, No. 9, 1966, pp. 1232–1242.

[2] Savic, P. and Stubbe, E., "Inductive Plasma Conductivity Probes," Mechanical Engineering Rept. Mt-56, May 1966, National Research Council of Canada, Ottawa.

[3] Vendell, E. W., "Boundary Corrections for a Three-Coil Conductivity/Velocity Plasma Probe," TN D-4538, April 1968, NASA.

[4] Anderson, L. A. and Sheldahl, R. E., "Flow-Swallowing Enthalpy Probes in Low-Density Plasma Streams," AIAA Paper 68–390, San Francisco, Calif. 1968.

[5] Emmons, H. W. and Land, R. I., "Poiseuille Plasma Experiment," *The Physics of Fluids*, Vol. 5, No. 12, 1962, pp. 1489–1500.

[6] Ahtye, W. F., "A Critical Evaluation of Methods for Calculating Transport Coefficients of Partially and Fully Ionized Gases," TN D-2611, Jan. 1965, NASA.

[7] Anderson, L. A., private communication: "Plot of h_{av} vs. I_{arc} for the Ames 1.27-cm-diameter TA constricted arc facility," Aug. 1968, NASA.